SEI Structural Engineering Institute of the American Society of Civil Engineers
2005 Structures Congress
Metropolis & Beyond

IDA Capacity Curves: The Need for Alternative Intensity Factors

Sashi K. Kunnath & Erol Kalkan

University of California Davis, Dept. of Civil and Env. Engineering

Presentation Outline:

1) Incremental-Dynamic-Analysis (IDA)

2) Evaluation study

- *Analytical model description*
- *Ground motion data set*
- *Typical response of steel-frame building to near-fault records*
- *NTH analyses results: Common Seismic demand parameters*
- *Correlation of IDA curves with observed response*
- *Common intensity measures (IMs) and their critical evaluation*

3) Alternative IM to account for system inelastic behavior

4) Conclusion

Six-Story Steel Moment-Frame Building (Burbank, CA)

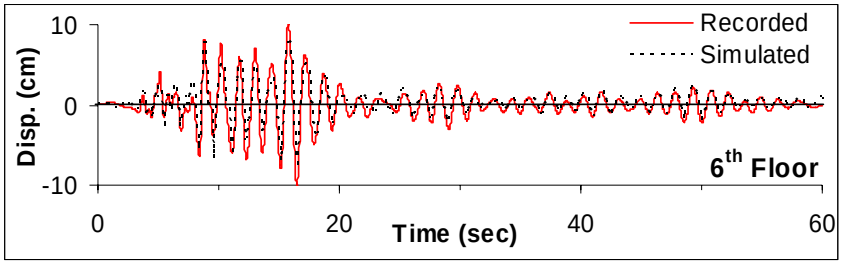

Comparison of recorded and computed response (a) at channel 2 (EW direction) at 6th storey level

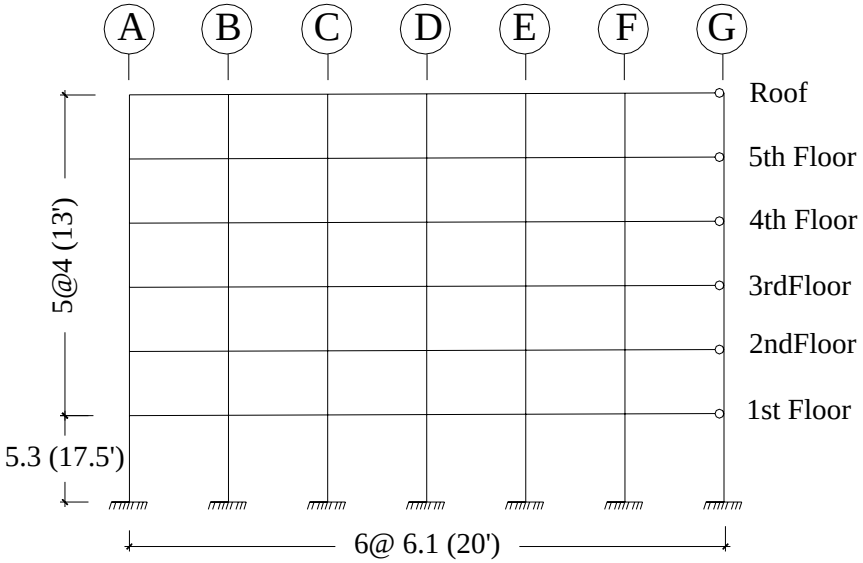

(a) Elevation view

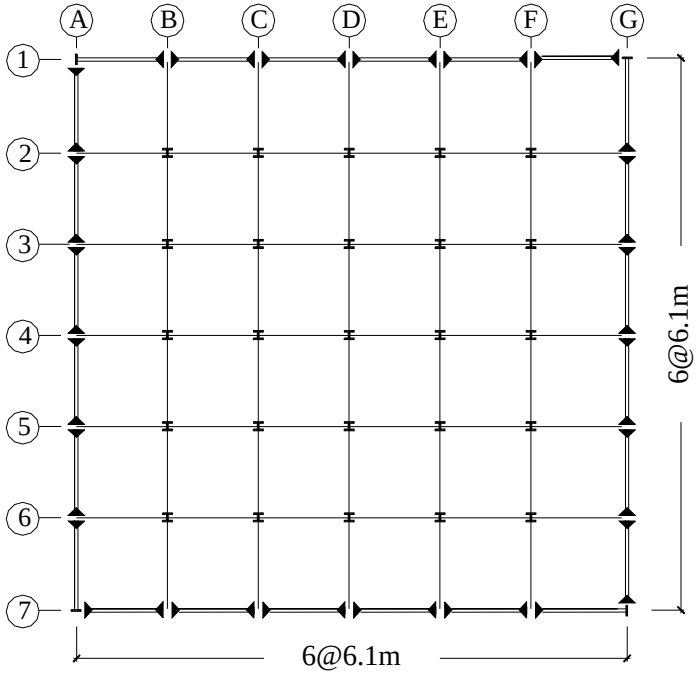

(b) Plan view

Ground Motion Database

No.	Year	Earthquake	M_W	Mech. *	Station	Component	Site Class	PGA (g)
(a) Far-Fault Recordings								
1	1952	Kern county	7.5	TH/REV	Taft	111	Soil	0.18
2	1979	Imperial-Valley	6.5	SS	Calexico	225	Soil	0.27
3	1989	Loma Prieta	7.0	OB	Cliff House	90	Stiff soil	0.11
4	1989	Loma Prieta	7.0	OB	Presido	0	Soil	0.19
5	1992	Big Bear	6.4	SS	Desert Hot	90	Soil	0.23
6	1994	Northridge	6.7	TH	Century	90	Soil	0.26
7	1994	Northridge	6.7	TH	Montebello	206	Soil	0.18
8	1994	Northridge	6.7	TH	Terminal Island	330	Soil	0.19
9	1994	Northridge	6.7	TH	SantaFE Spr.	30	Soil	0.14
10	1994	Northridge	6.7	TH	Saturn	S70E	Soil	0.43
(b) Near Fault Recordings (Forward-Rupture Directivity)								
1	1989	Landers	7.3	SS	Lucerne	275	Stiff soil	0.721
2	1989	Loma Prieta	7.0	OB	Lexington Dam	90	Stiff soil	0.41
3	1989	Loma Prieta	7.0	OB	LGPC	0	Stiff soil	0.56
4	1992	Cape Mendocino	7.1	TH	Petrolia	90	Stiff soil	0.66
5	1992	Erzincan	6.7	SS	Erzincan	EW	Soil	0.50
6	1994	Northridge	6.7	TH	Rinaldi	275	Soil	0.84
7	1994	Northridge	6.7	TH	Olive View	360	Soil	0.84
8	1994	Northridge	6.7	TH	Slymar Converter	018	Soil	0.83
9	1995	Kobe	6.9	SS	KJMA	0	Stiff soil	0.82
10	2003	Bingol	6.4	SS	Bingol	NS	Soil	0.56

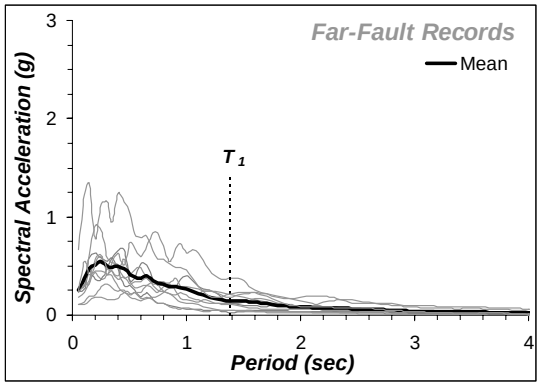

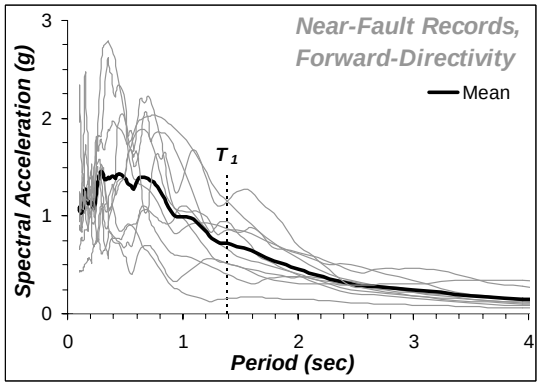

Pseudo-spectral acc. spectra and mean spectra of far-fault and near-fault records

Ten ordinary far-fault and ten near-fault records are used in IDA study.

Near-fault records are characterized by forward-directivity, and exhibit coherent-long period velocity pulses.

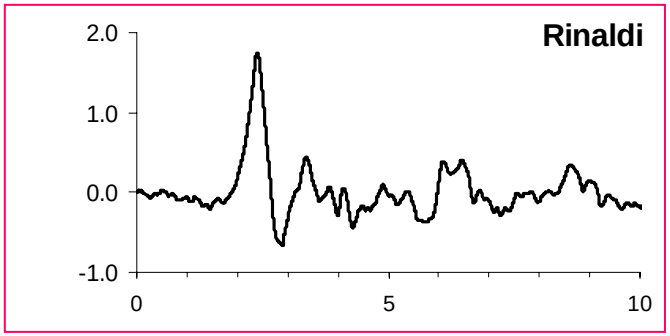

Six-Story Building Response to Typical Near-Fault Ground Motions

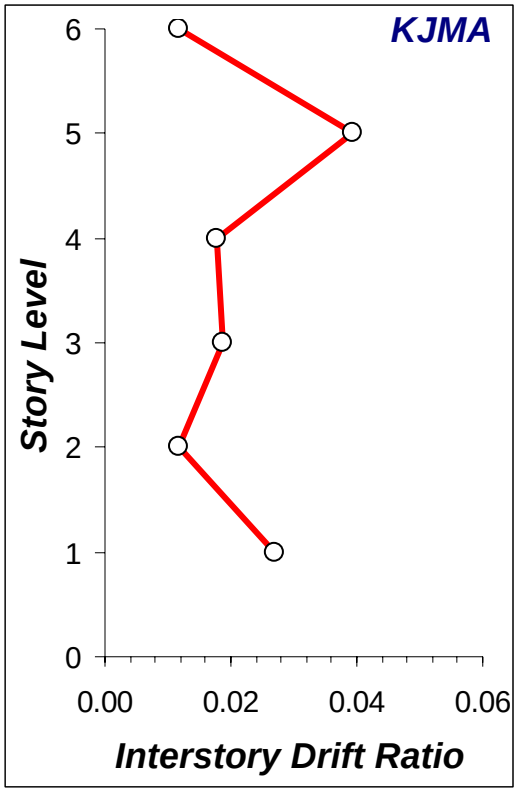

Response dominated by higher modes

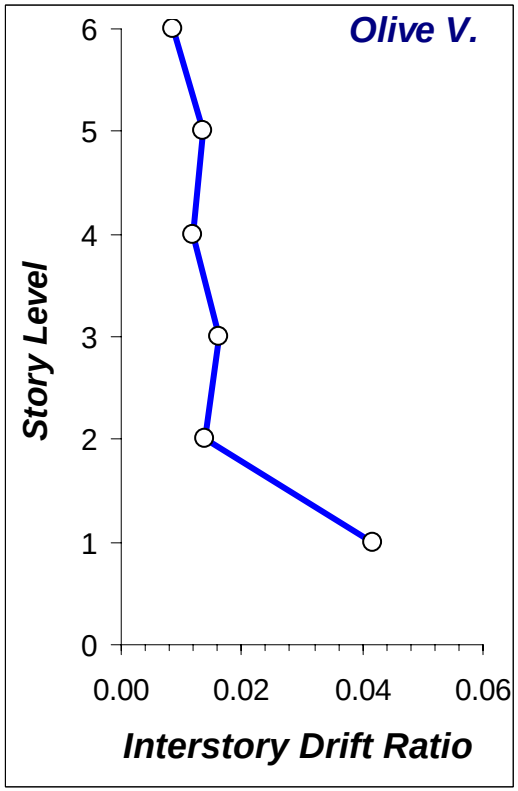

Response dominated by first mode

NTH Analysis Results: Far-Fault and Near-Fault Records

Mean and 84 percentile curves: Roof drift ratio; Inter-story drift ratio; Story ductility

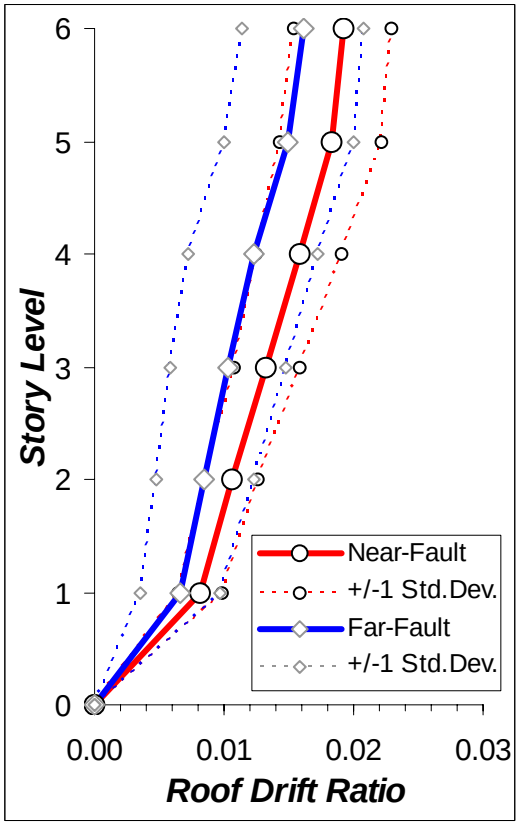

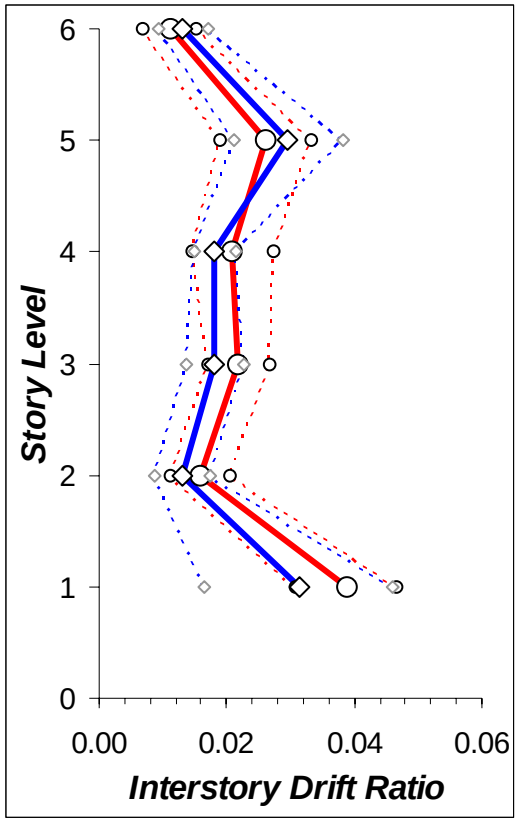

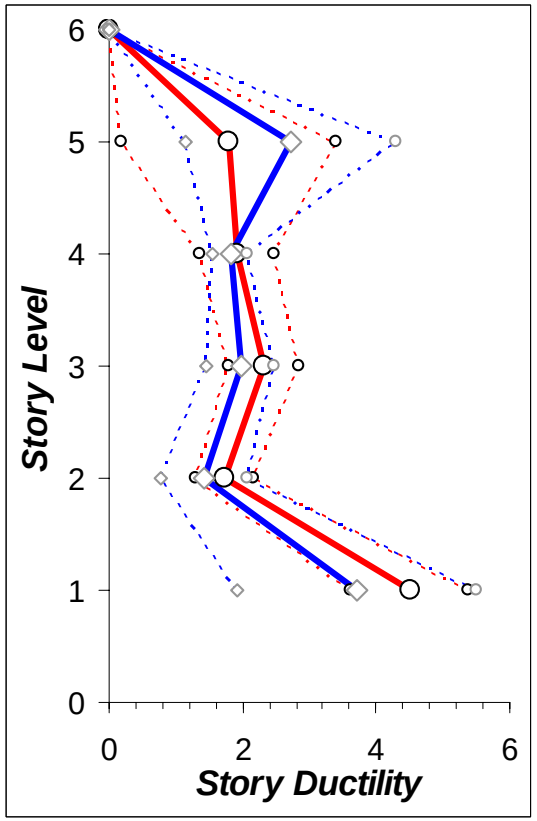

- **Largest demand concentrated at first and fifth story levels showing large interstory drift.**
- **While the dispersion is almost similar, near-fault records yielded larger demand.**

Progressive change in interstory drift and story ductility demands during IDA analysis

Far-Fault Record

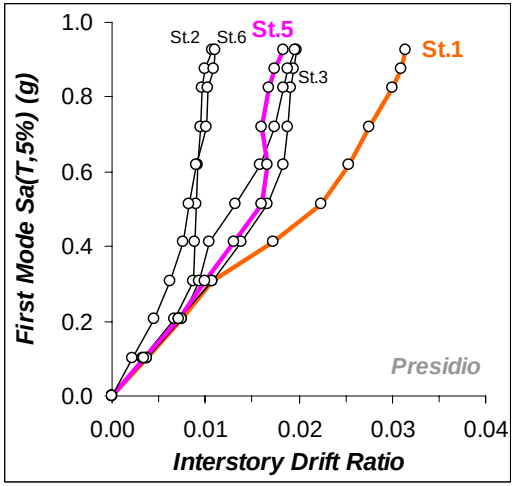

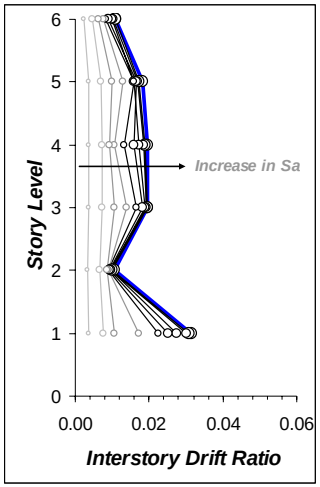

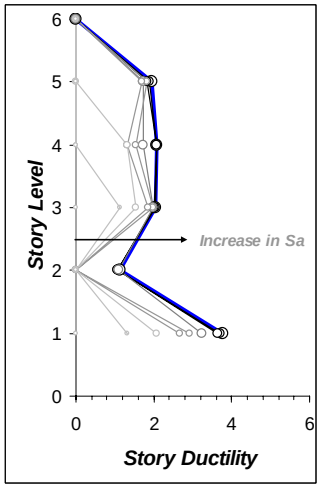

Near-Fault Record

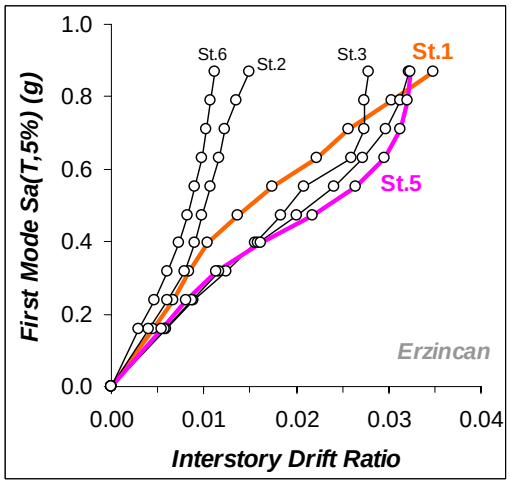

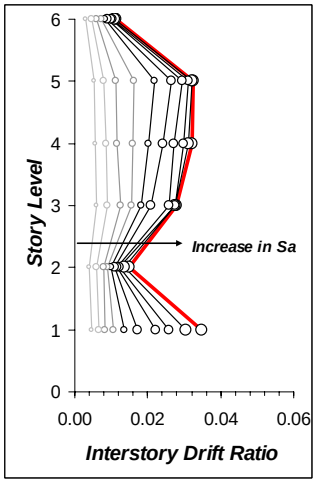

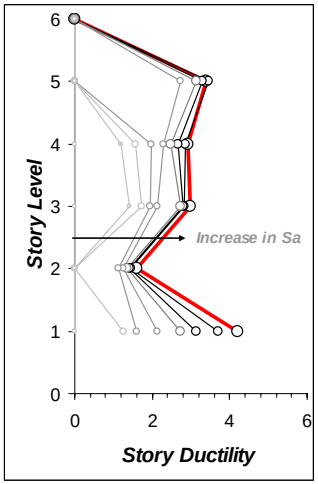

- IDA curves show hardening being inconsistent with the observed inelastic response

Variation of base shear coefficient with increase in $S_a(T_1,5\%)$

Far-Fault Records

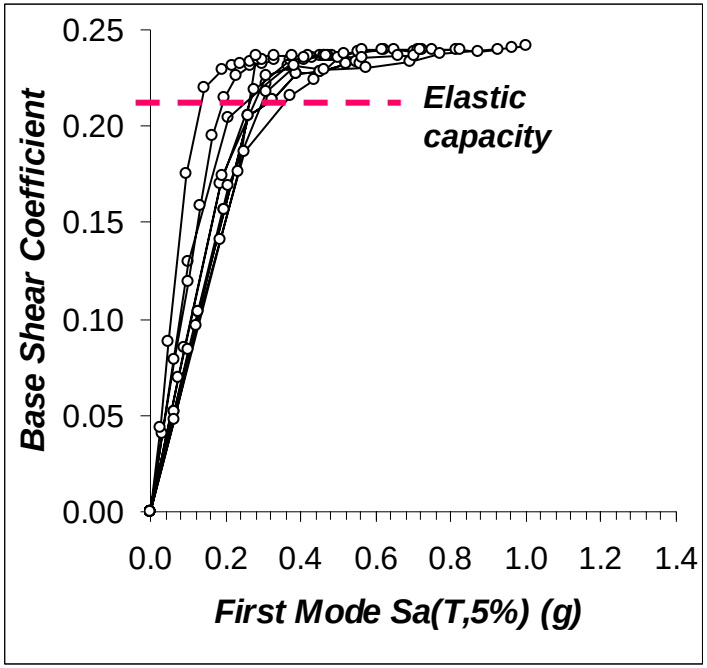

Near-Fault Records

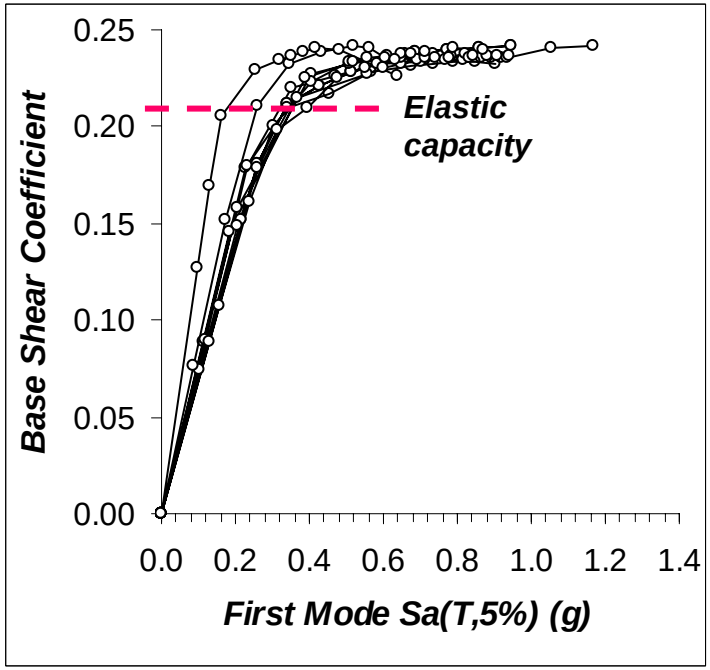

IDA curves plotted as a function of base shear coefficient

Far-Fault Records

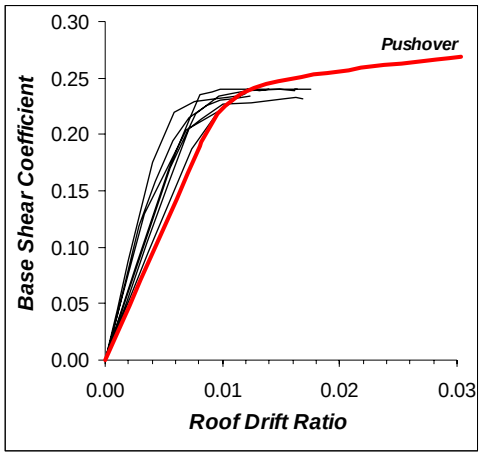

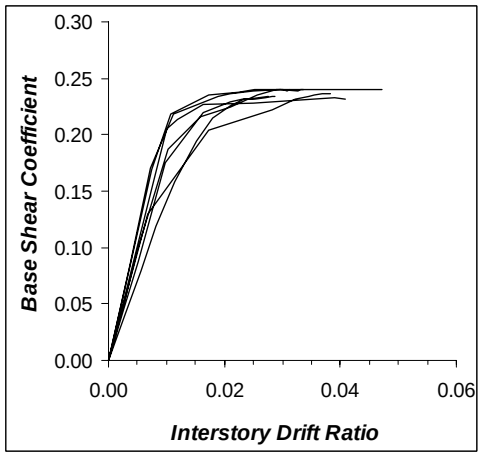

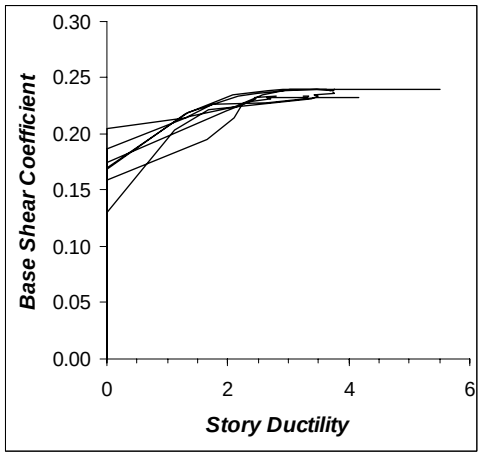

Near-Fault Records

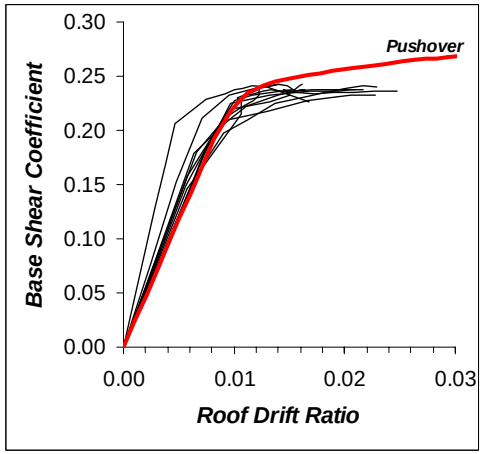

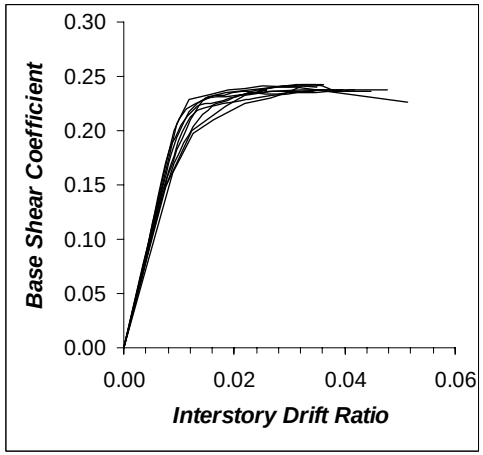

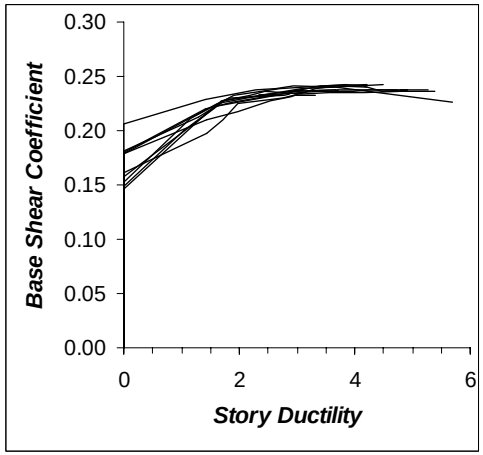

- **Base shear coefficient during IDA analyses are well correlated with static pushover analysis**

Common Intensity Measures

	Intensity Measure	Unit	Definition
1	Peak ground acceleration	g	PGA
2	Peak ground velocity	cm/sec	PGV
3	First mode spectral acceleration	g	$\mathrm{PSA}(T_1, \delta)$
4	Root mean square acceleration	g	$A_{rms} = \sqrt{\frac{1}{T_D}\int_0^D [\ddot{u}_g(t)]^2\, dt}$
5	Cordova predictor	g	$IM_{1eff} = S_a(T_1,\xi)\left[\frac{S_a(cT_1,\xi)}{S_a(T_1,\xi)}\right]^{\alpha}, c = 2; \alpha = 0.5$
6	Effective peak acceleration [ATC 3-06, 1978]	g	$EPA = \frac{S_{a,avg}(T_1,\xi)\Big\|_{0.1}^{0.5}}{2.5}$

IM-1: IDA curves plotted against PGA

Far-Fault Records

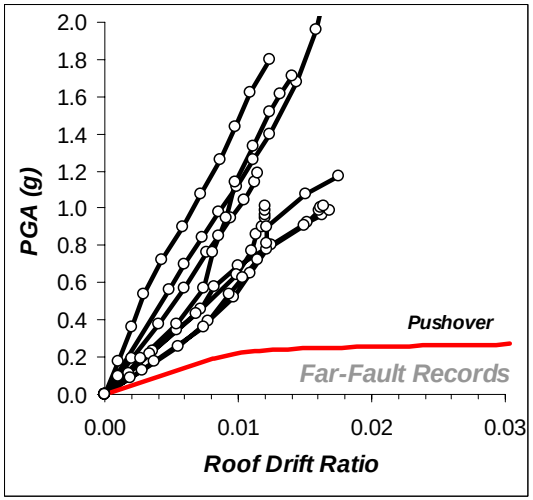

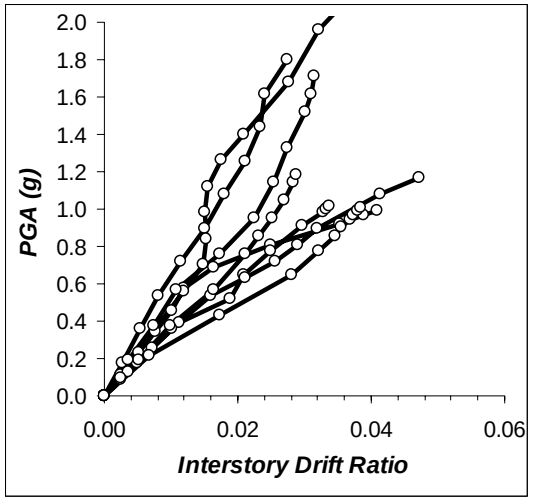

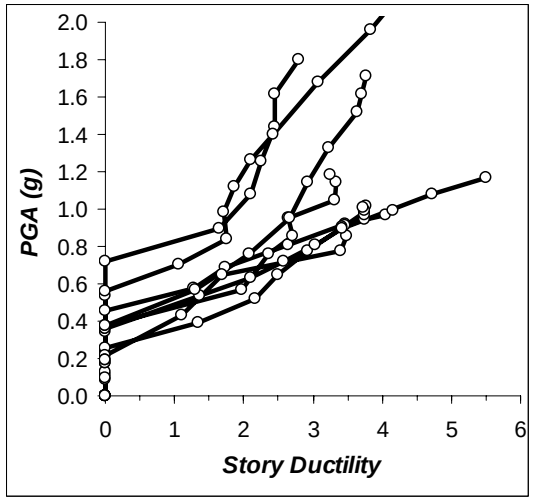

Near-Fault Records

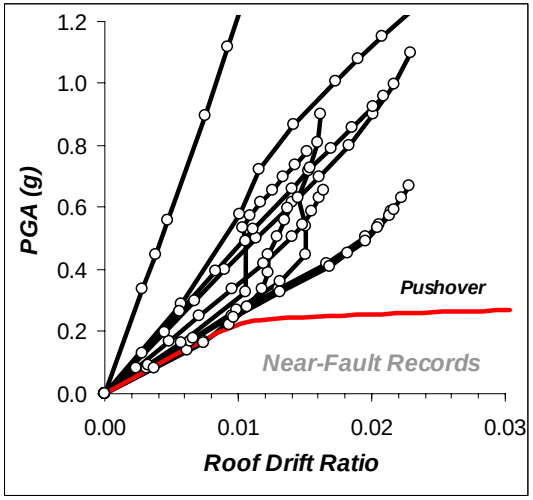

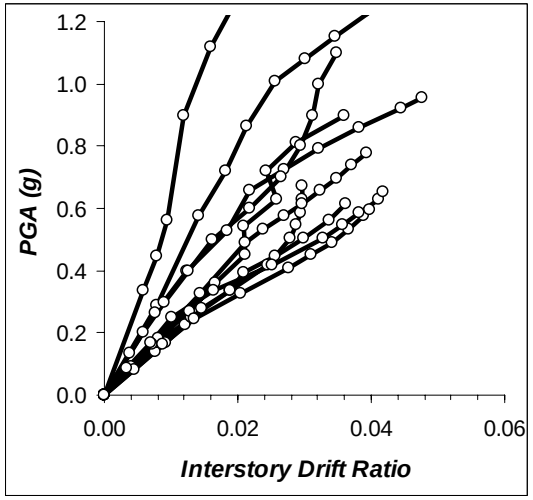

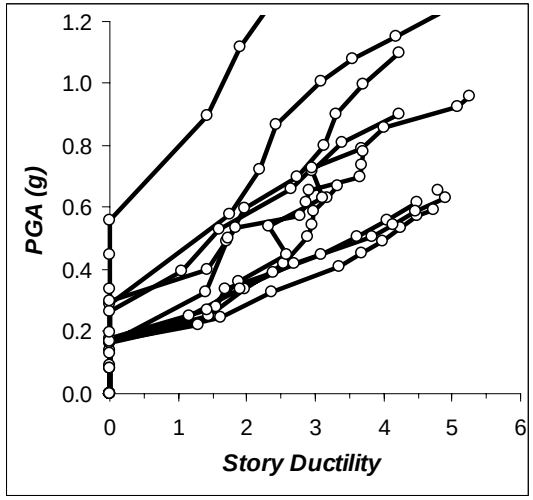

IM-2: IDA curves plotted against PGV

Far-Fault Records

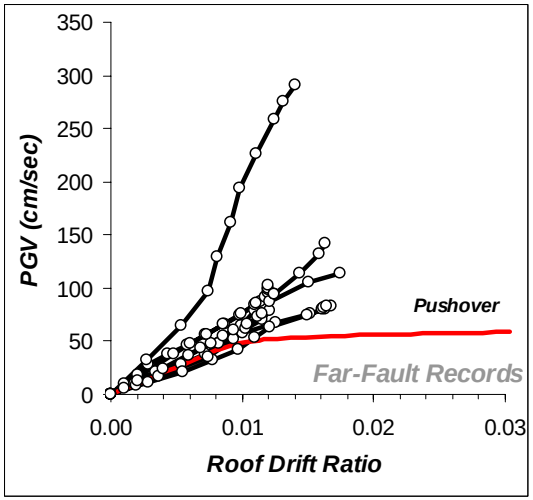

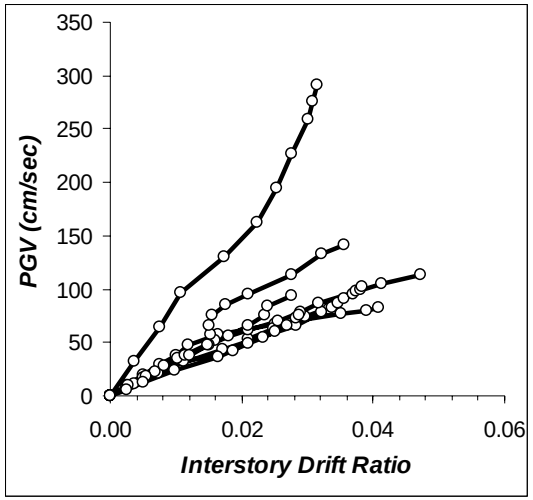

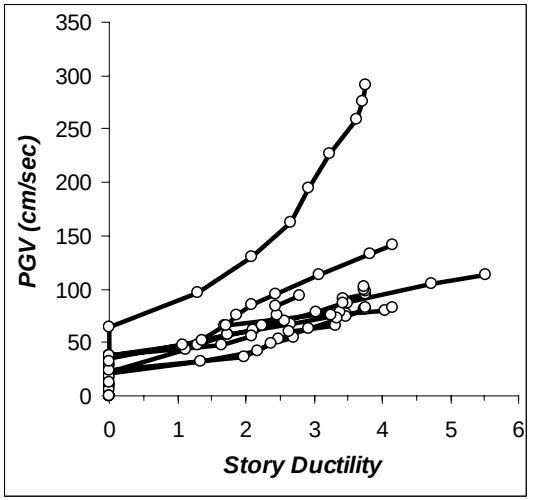

Near-Fault Records

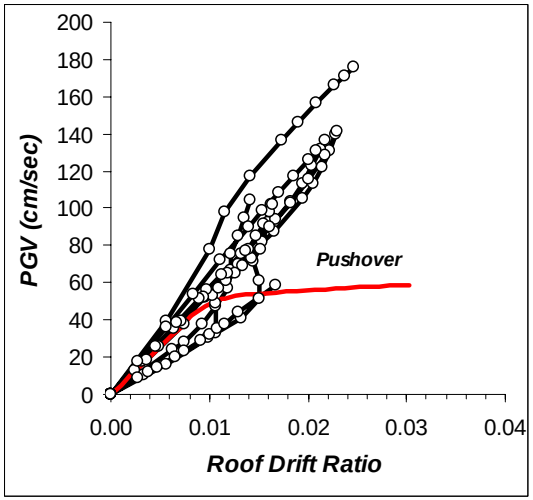

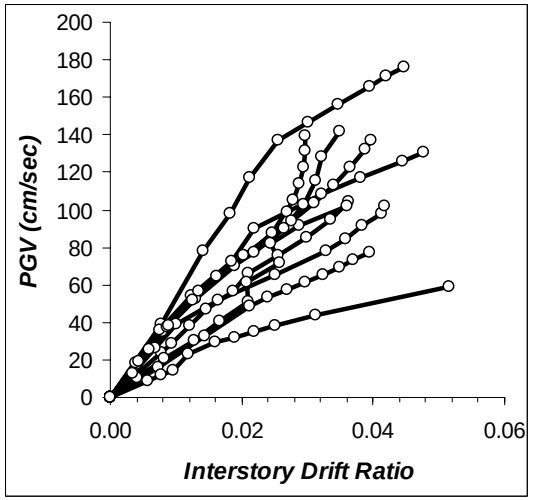

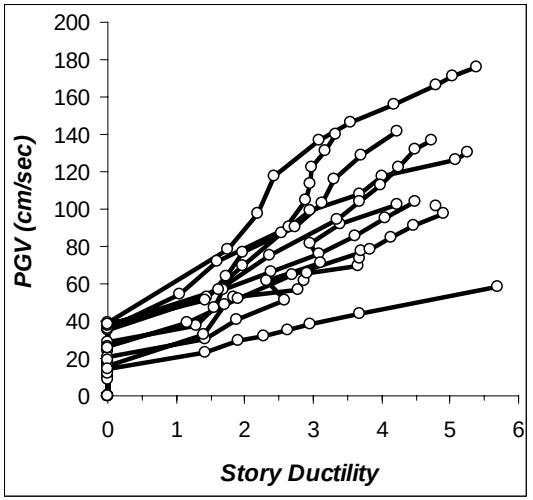

IM-3: IDA curves plotted against $Sa(T_1, 5\%)$

Far-Fault Records

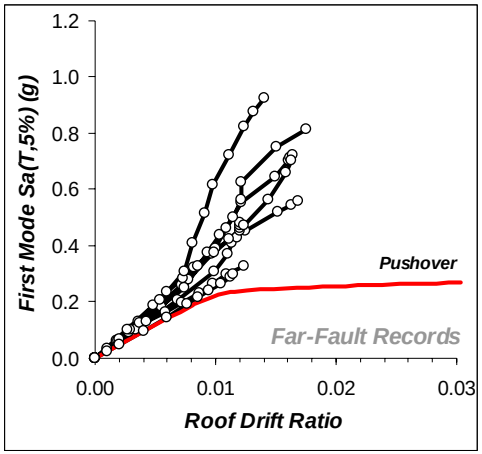

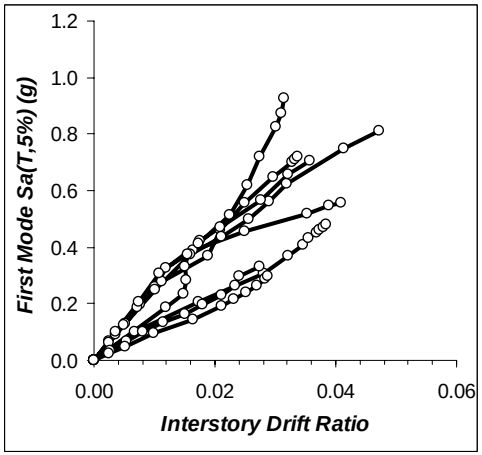

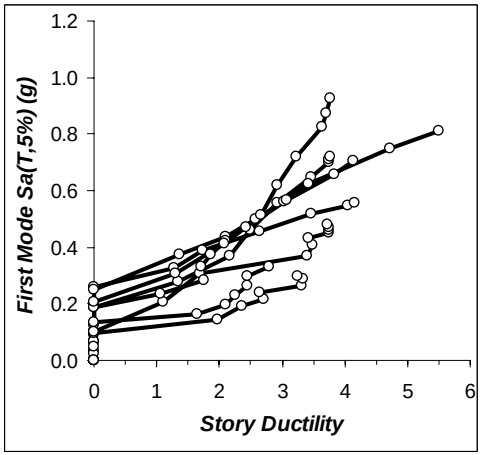

Near-Fault Records

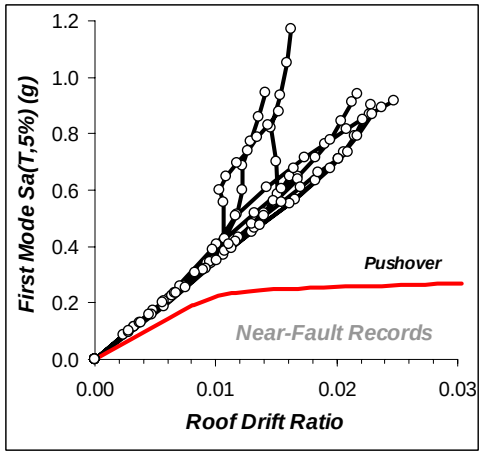

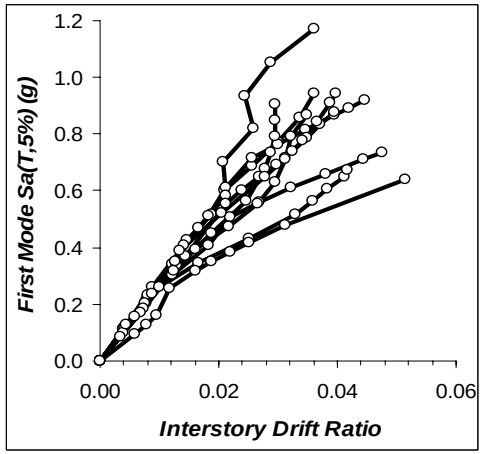

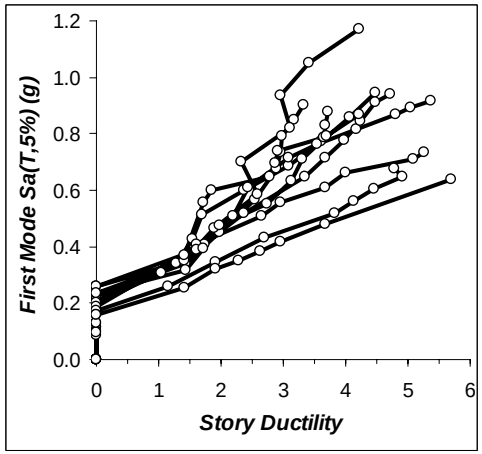

IM-4: IDA curves plotted against RMS-Acc.

$$A_{rms} = \sqrt{\frac{1}{T_D}\int_0^D [\ddot{u}_g(t)]^2 dt}$$

Far-Fault Records

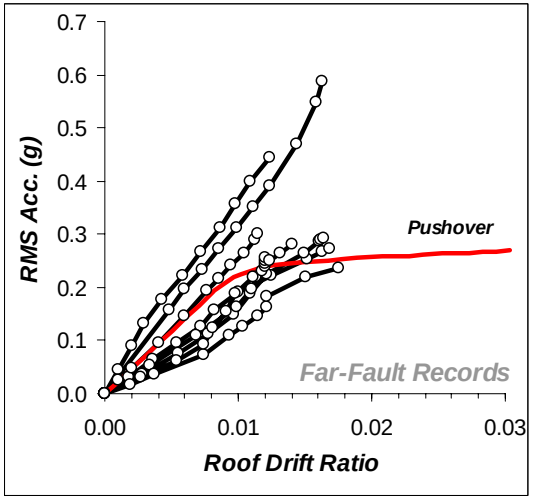

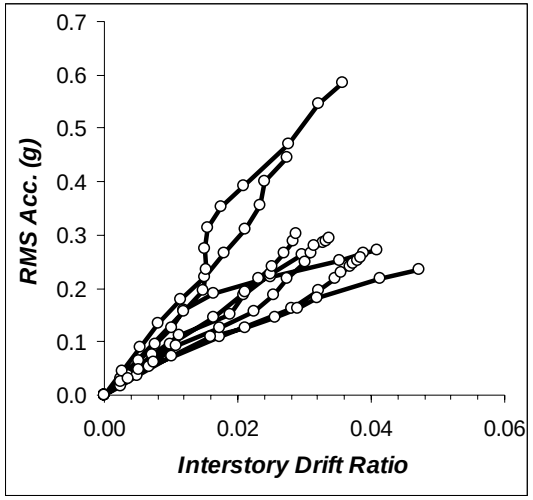

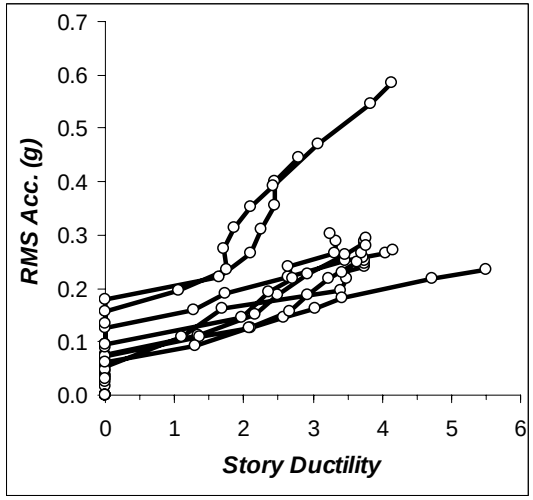

Near-Fault Records

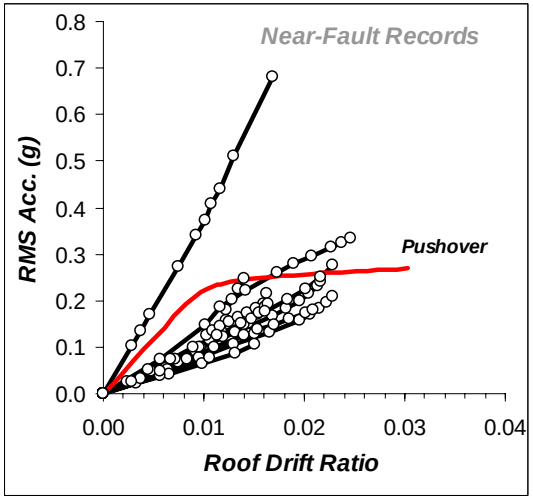

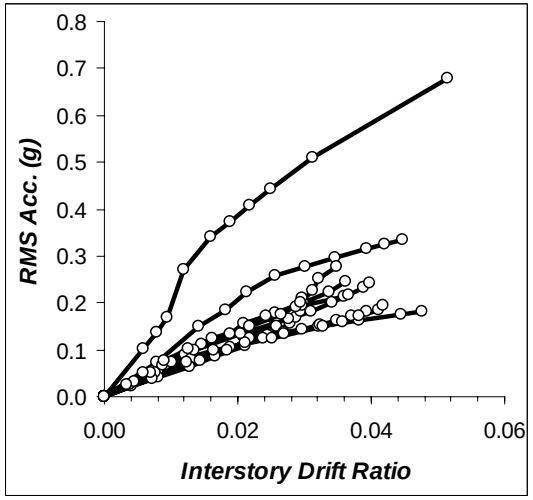

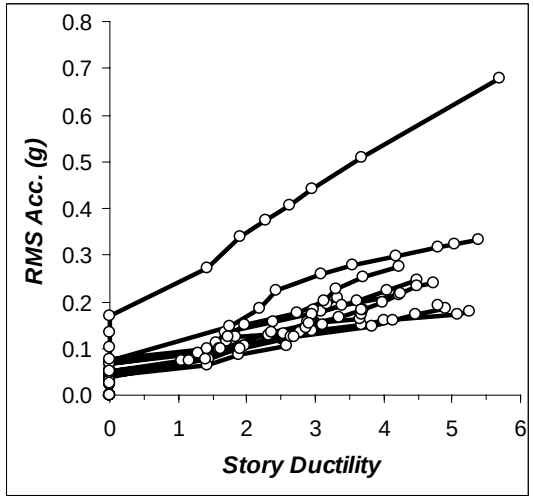

IM-5: IDA curves plotted against Cordova Predictor

$$IM_{1eff} = S_a(T_1,\xi)\left[\frac{S_a(cT_1,\xi)}{S_a(T_1,\xi)}\right]^{\alpha}, c = 2; \alpha = 0.5$$

Far-Fault Records

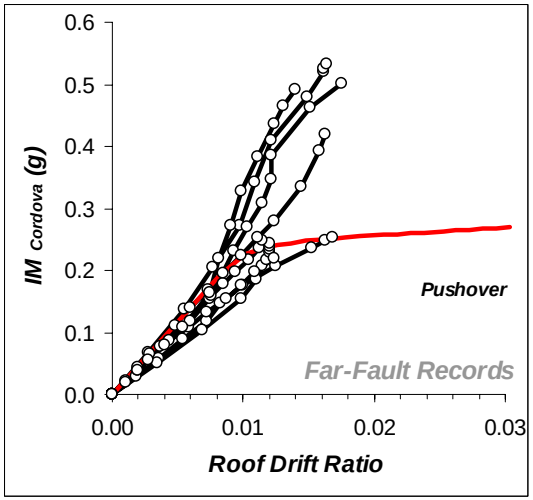

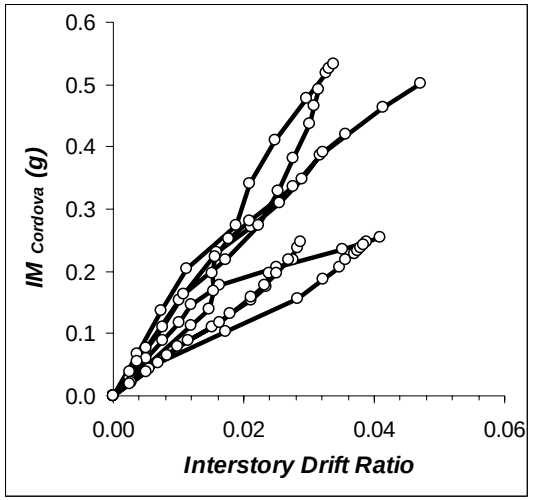

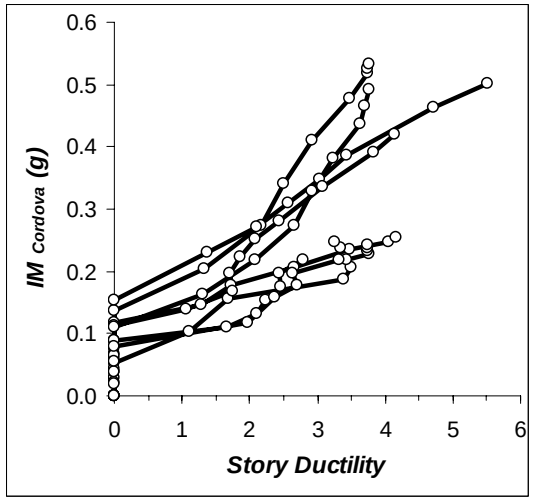

Near-Fault Records

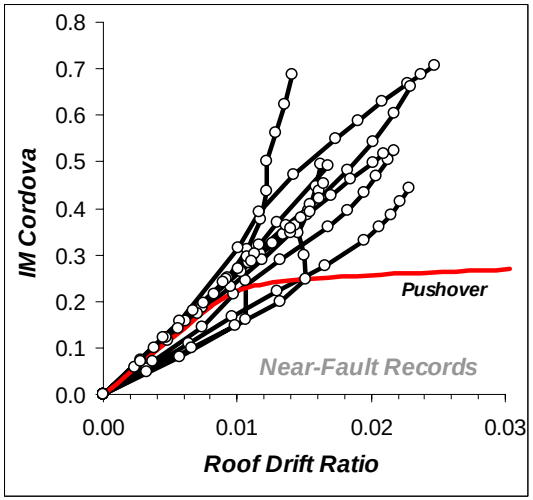

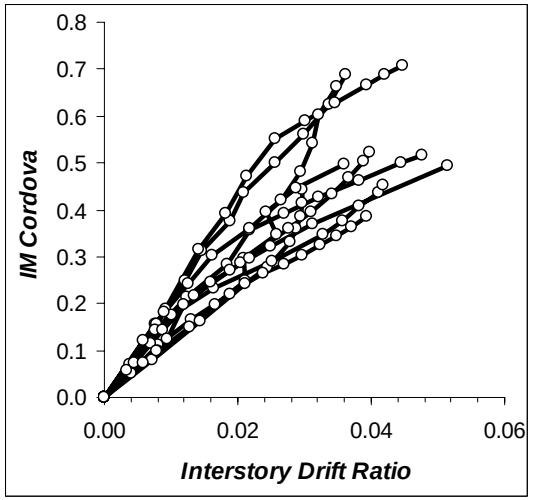

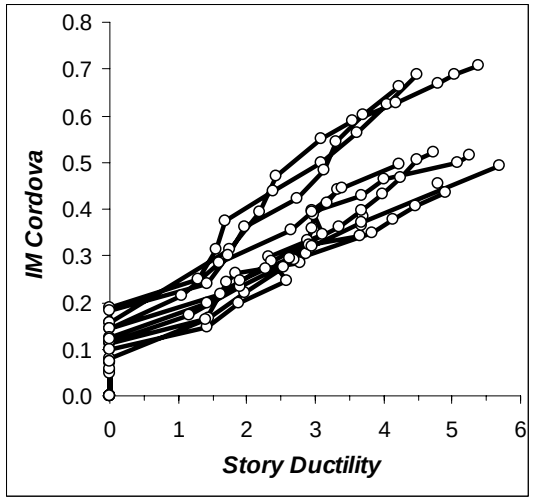

IM-6: IDA curves plotted against EPA

$$EPA = \frac{S_{a,avg}(T_1, \xi)\Big|_{0.1}^{0.5}}{2.5}$$

Far-Fault Records

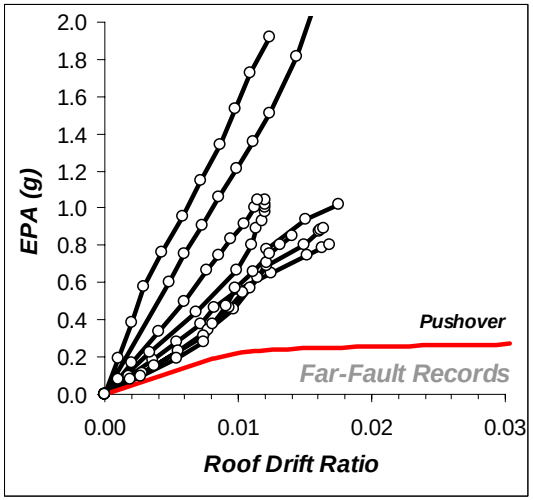

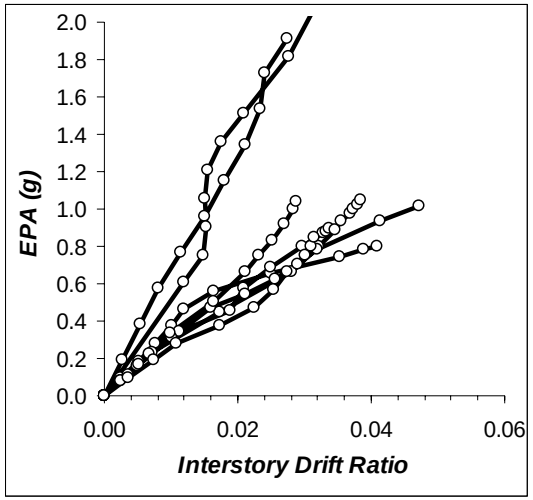

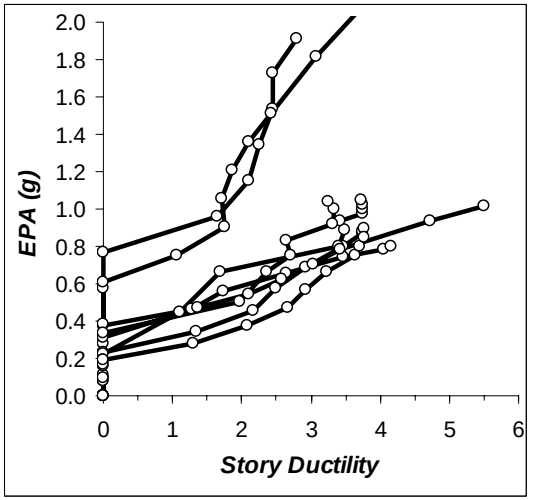

Near-Fault Records

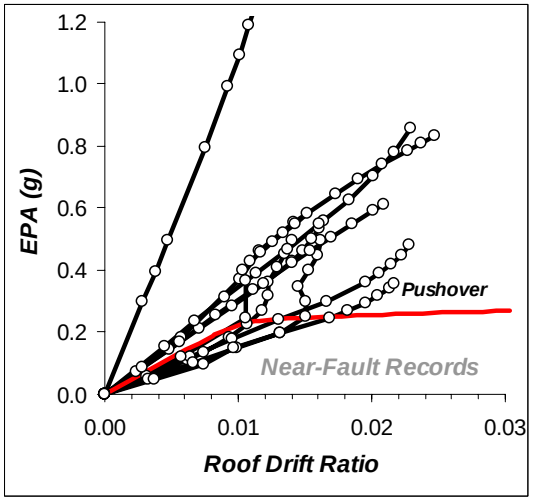

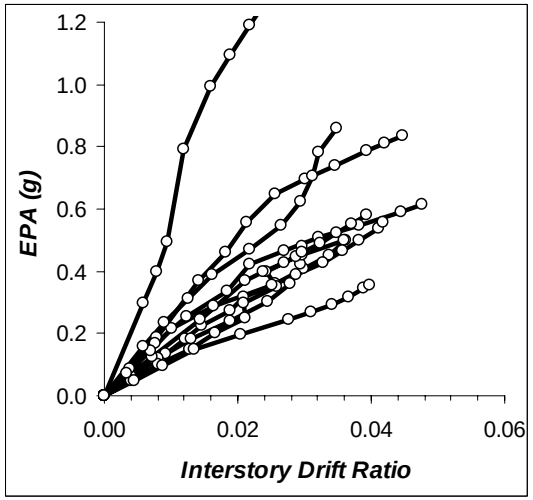

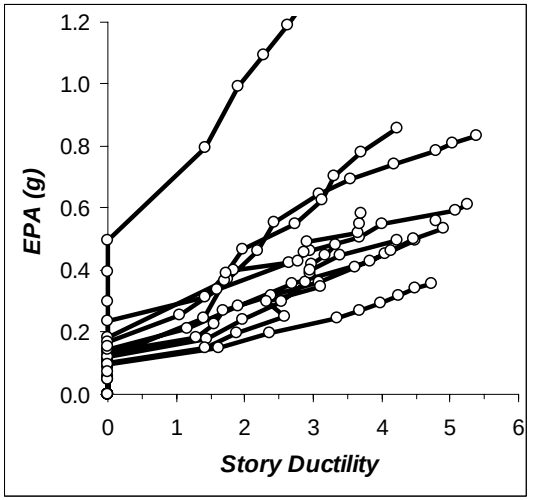

IM-3: IDA curves plotted against $S_a(T_1, 5\%)$

1st Story Peak
4th Story Peak
5th Story Peak

Far-Fault Records

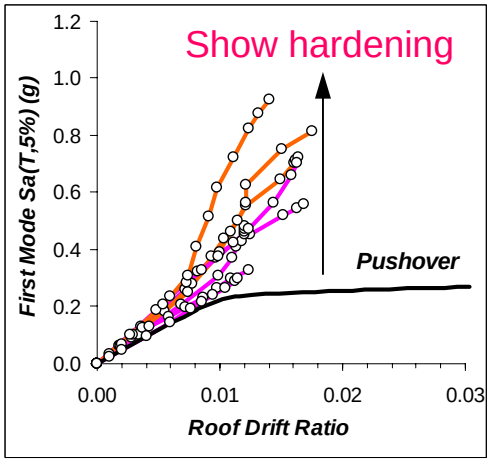

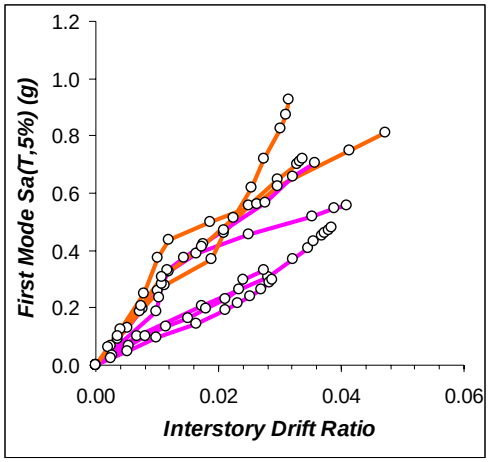

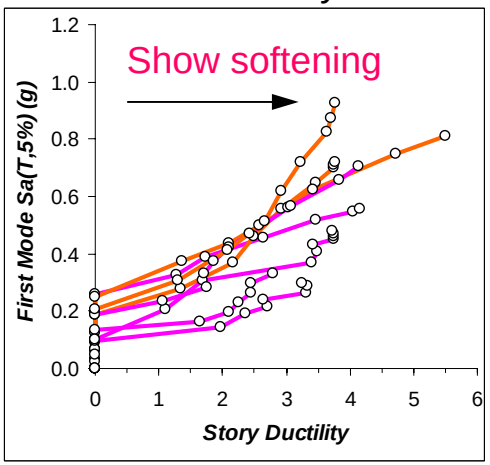

Near-Fault Records

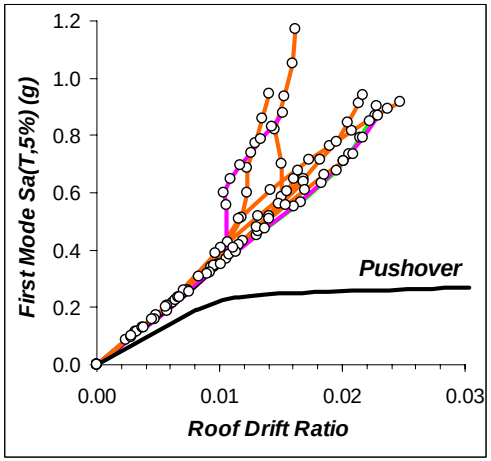

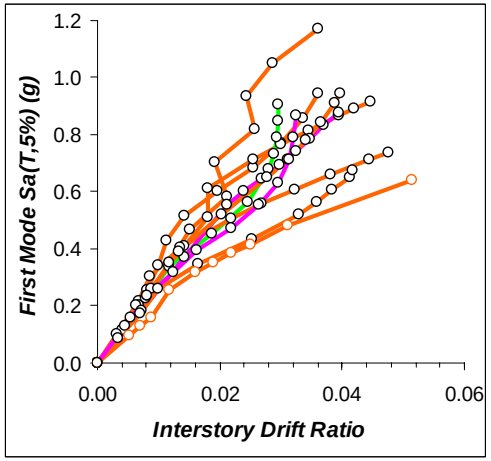

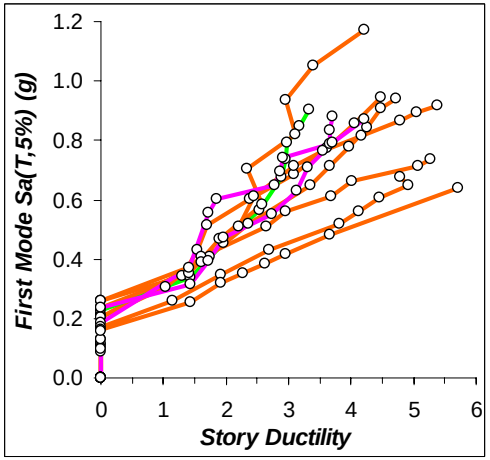

- **Long period pulses contained in NF records dominantly triggered the first mode response**

Progressive change in fundamental period (T_1) during inelastic response

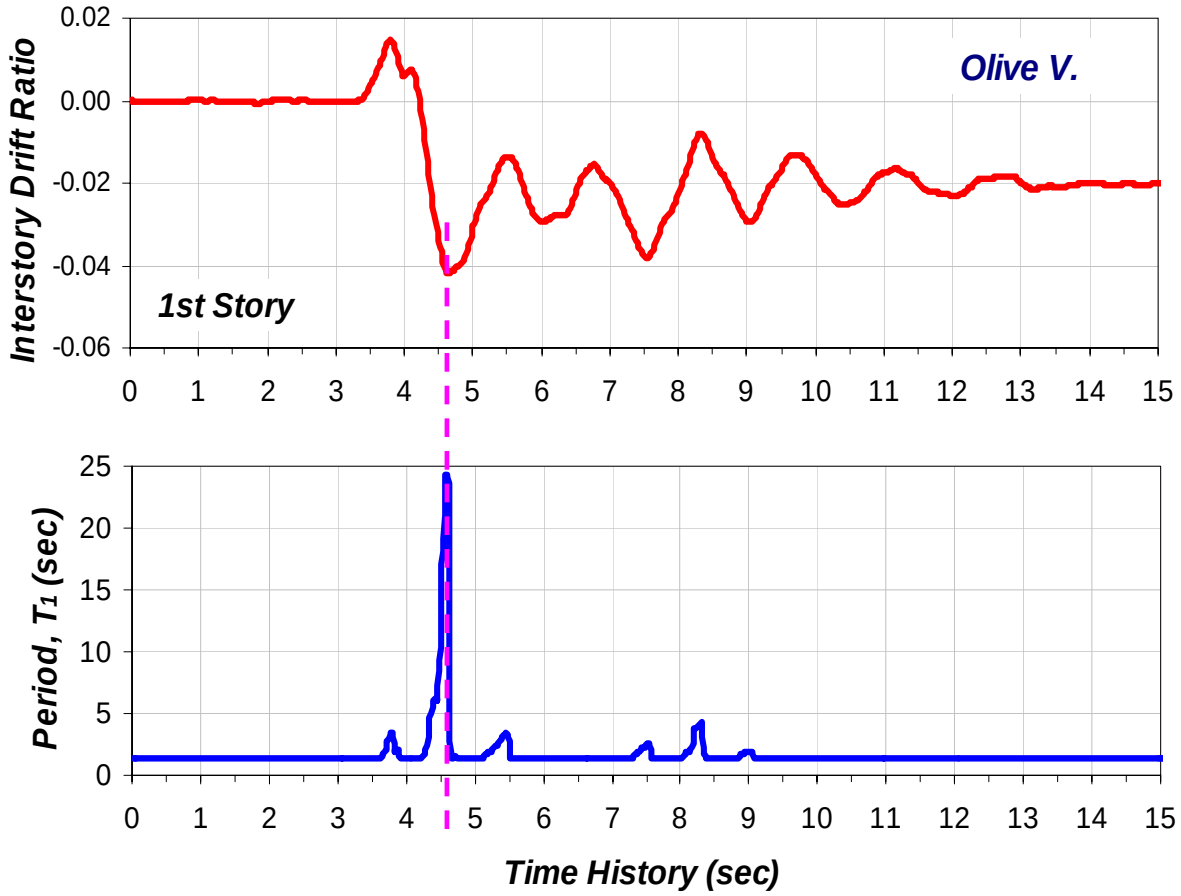

- In the inelastic range, the period of building deviates dramatically from its elastic counterpart

An Alternative Intensity Measure, Accounting for Inelastic Response

An IM based on inelastic spectral acceleration is used to account for change in system attributes during inelastic response.

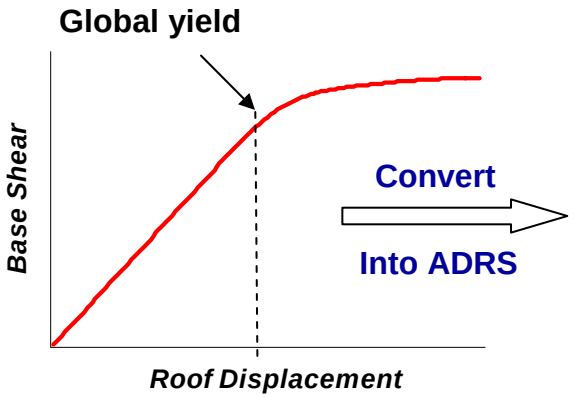

Capacity curve from static pushover

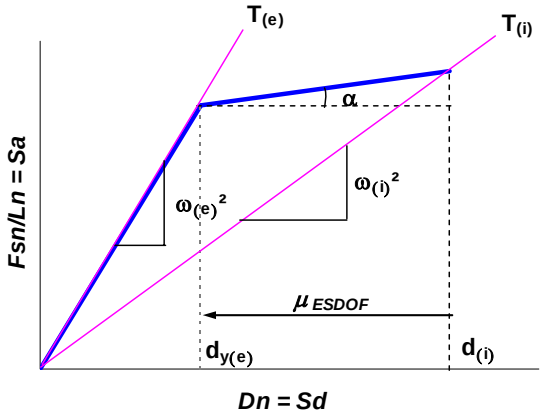

ADRS Format (ESDOF)
[after ATC-40 Linearization]

Correlation of secant period to ESDOF ductility:

$$\omega^2_{(inelastic)} = \frac{\alpha(\mu_{ESDOF} - 1) + \omega^2_{(elastic)}}{\mu_{ESDOF}}$$

Explicit representation of secant period

- By using the global yield point approximated from static pushover, system ductility can be computed at any level of IDA
- With approximated ductility, secant period is obtained from ESDOF representation
- Inelastic spectrum is generated with known ductility
- IM based on inelastic spectral acceleration is obtained with known secant period

IM Based on Inelastic Spectrum and ESDOF System Secant Period: Preliminary Results

Far-Fault Record

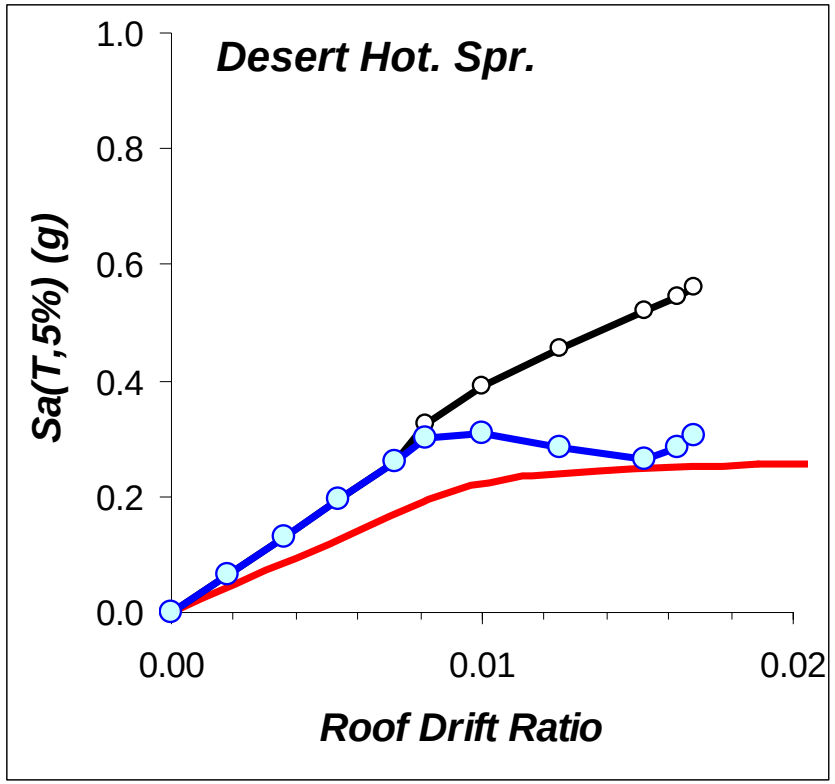

Near-Fault Record

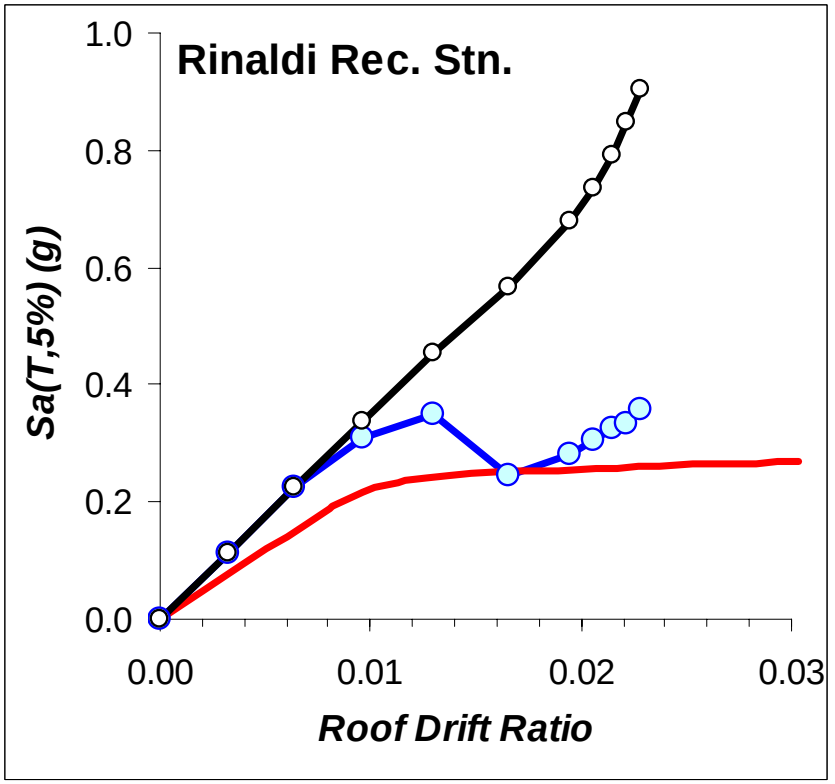

Conclusions

1) *Evaluation of the most common IMs for six-story steel building showed that there exist significant dispersion and none of the IMs are well correlated to the inelastic system behavior.*

2) *There is therefore a need for alternative IM to be used in performance-based engineering.*

3) *The IM based on inelastic spectrum and ESDOF secant period seems was developed, and tested using a near-fault and far-fault records.*

4) *On the basis of preliminary results, IM utilizing inelastic spectral acceleration seems to be promising. A more comprehensive evaluation considering different seismic source characteristics and building models is currently underway*